Genomics 95 (2010) 16–24

Contents lists available at ScienceDirect

Genomics

journal homepage: www.elsevier.com/locate/ygeno

Integrated molecular analysis suggests a three-class model for low-grade gliomas: A proof-of-concept study

Nicholas F. Marko [a,*], Richard A. Prayson [c], Gene H. Barnett [a,b], Robert J. Weil [a,b,*]

[a] Department of Neurosurgery, The Cleveland Clinic, Cleveland, OH, USA
[b] Brain Tumor and Neuro-Oncology Center, Neurological and Taussig Cancer Institutes, The Cleveland Clinic, Cleveland, OH, USA
[c] Department of Pathology, The Cleveland Clinic, Cleveland, OH, USA

ARTICLE INFO

Article history:
Received 23 June 2009
Accepted 29 September 2009
Available online 14 October 2009

Keywords:
Glioma
Low grade
Classification
Gene expression
Genomics
Microarray

ABSTRACT

Introduction: We used an integrated molecular analysis strategy to perform class discovery on a population of low-grade gliomas (astrocytomas, oligodendrogliomas, and mixed gliomas) to improve our understanding of the molecular relationships among these tumors and to reconcile genotypic relationships with current histologic and molecular strategies for tumor classification.

Methods: Gene expression profiling was performed on a cross-section of World Health Organization (WHO) grades I–II gliomas. Unsupervised class discovery algorithms identified and validated tumor clusters with genotypic similarity, and these data were integrated with chromosomal copy number assays and RT-PCR data to define molecular tumor subclasses. Machine learning models allowed accurate, prospective classification of unknown tumors into these molecular subgroups. This molecular classification model was compared to current histologic (WHO) and molecular pathologic (chromosome 1p and 19q deletions, p53 alterations, and Ki-67 expression) methods for glioma classification.

Results: Molecular class discovery suggested a three-class model for low-grade gliomas. One discrete cluster of gliomas identified the pilocytic astrocytomas, a second grouped the 1p/19q codeleted oligodendrogliomas, and the mixture of remaining 1p/19q intact gliomas, including astrocytomas, oligodendrogliomas, and oligoastrocytomas, formed a third cluster with a discrete pattern of expression.

Conclusions: Integration of genomic, transcriptomic, and morphologic data for class discovery suggests a three-class model for low-grade gliomas. Class I represents tumors with molecular similarity to pilocytic astrocytomas, class II tumors are similar to 1p/19q codeleted oligodendrogliomas, and class III represents infiltrative low-grade gliomas. This classification is similar to current clinical paradigms for low-grade gliomas; our work suggests a molecular basis for such models. This classification may supplement or may serve as the basis for a molecular pathologic alternative to current grading schemes for low-grade gliomas and may highlight potential targets for future biologically based treatments or strategies for future clinical trials.

Introduction

Each year, approximately 30,000 patients are diagnosed with central nervous system (CNS) gliomas. The majority of these tumors are classified as high-grade (malignant) gliomas, a collective term that encompasses anaplastic astrocytoma, anaplastic oligoastrocytoma and anaplastic oligodendroglioma (WHO grade III tumors), as well as gliosarcoma and glioblastoma (WHO grade IV tumors) [1]. Regardless of the histologic subtype, treatment of these patients is similar (surgical resection + radiation ± chemotherapy) and survival is generally short (1–5 years) [2–4]. Gliomas with less malignant histologic appearance are classified into WHO grades I–II. The histologic classification schema for these "low-grade gliomas" is complex, using morphologic features, which may be inconsistent or subject to variable interpretation, to assign tumors to several categories, and include astrocytoma (pilocytic, pilomixoid, fibrillary, gemistocytic, protoplasmic), oligodendroglioma, mixed glioma (oligoastrocytoma), and subependymal giant cell astrocytoma (SEGA) [1]. While assignment to select WHO classes (i.e., pilocytic astrocytoma, SEGA) has specific implications for treatment and prognosis, the WHO class for most grades I–II gliomas does not reflect major phenotypic differences. From a biological perspective, it has been difficult to determine to what degree the WHO classification accurately reflects underlying tumor cell biology.

The relative rarity of these tumors and the prolonged survival of patients diagnosed with these lesions (5–20^{+} years after diagnosis)

* Corresponding authors. N.F. Marko is to be contacted at Department of Neurosurgery, Cleveland Clinic, Desk ND-409500 Euclid Avenue, Cleveland, OH 44195, USA. Fax: +1 216 636 0454. R.J. Weil, Brain Tumor and Neuro-Oncology Center, Neurological Institute, Cleveland Clinic, 9500 Euclid Avenue, Cleveland, OH 4419, USA.
E-mail address: markon@ccf.org (N.F. Marko).

0888-7543/$ – see front matter © 2009 Elsevier Inc. All rights reserved.
doi:10.1016/j.ygeno.2009.09.007

complicate subgroup identification and evidence-based research for low-grade gliomas, which limits large-scale, prospective trials of treatment strategies [1]. Given sparse data, nearly all combinations of observation, biopsy, surgical resection, and adjuvant therapy have been advocated for management of patients with such tumors [5], resulting in variable outcomes. A cycle develops, as multiple treatment strategies are inconsistently applied to small subsets of patients with low-grade gliomas, further limiting the ability to conduct meaningful outcomes research. Accordingly, consensus regarding optimal, biologically based management of most patients with WHO grades I–II gliomas is lacking [5].

This problem highlights the need for a classification system for low-grade gliomas that reflects tumor biology and that can be used prospectively to guide clinical trial design and patient management. A molecular classification system based upon the tumor transcriptome is an attractive option [6,7], because phenotype is associated with genotype. Molecular classification using microarray expression profiles has been investigated in pilocytic astrocytomas [8] and in high-grade gliomas by ourselves [9] and others [10–16], and these studies have identified molecular subgroups with divergent phenotypes (including patient survival), often within a single WHO grade [5,9]. Applying a similar approach to low-grade gliomas may identify molecular subclasses of these tumors with prognostic and therapeutic significance.

Because WHO grades I–II gliomas are significantly less common than high-grade gliomas, availability of tissue for histologic and molecular analysis has made such investigations more difficult than similar research for high-grade gliomas. A detailed review by Rorive et al. [17] summarized the genomic literature for low-grade astrocytomas to date, citing only 11 studies [12,18–27] that have collected "sound [expression] data" [17] for these tumors. This literature tends to be descriptive, enumerating genes that are differentially expressed between low-grade gliomas and normal brain [8,12,18,19,21,22,24,26,27] or between low-grade gliomas and their high-grade counterparts [12,19–21,23–25]. While such investigations can identify genes that may be markers of malignant progression in gliomas, these analyses have been limited in their ability to discover novel molecular subclasses or to classify unknown tumor samples into such classes in a prospective fashion. We believe that an unbiased investigation of low-grade gliomas, focused on identification and characterization of molecular subgroups, will further the understanding of the underlying biology of these tumors, will stimulate continued exploration of the WHO classification system, and will help establish a theoretical framework in which future attempts to correlate genotype and phenotype can be performed.

In this study, we examine the molecular relationships among a group of 23 tumors representing a cross-section of WHO grades I–II gliomas. We have constructed an integrative data analysis model that limits prospective biases, incorporates genomic, transcriptomic, and histologic data, and facilitates unbiased class discovery based on this integrated molecular data. Our aim is to improve our understanding of the relationships among these tumors and to reconcile these relationships with current histologic and molecular strategies for the classification of low-grade gliomas.

Materials and methods

Inclusion criteria

Patients selected for inclusion in this study had a confirmed diagnosis of WHO grades I–II glioma (pilocytic astrocytoma, diffuse astrocytoma, oligodendroglioma, or mixed glioma) [1]. Because of the tendency of these tumors to affect young people, patients of any age with the appropriate diagnosis were included. Tissue samples were obtained during initial tumor resections performed at our institution between August 2001 and August 2007 as part of standard medical management. Patients undergoing prior stereotactic biopsy were eligible for inclusion, but patients with prior tumor resections or prior management with chemotherapy and/or radiotherapy were excluded. Patients were also excluded if the available clinical information was insufficient to verify study eligibility or if the pathologic specimen was inadequate for microarray analysis.

Sample selection

This study was approved by the Cleveland Clinic Institutional Review Board. The Brain Tumor and Neuro-Oncology Center database was queried to generate a list of all patients meeting the inclusion criteria. The electronic medical records of these patients were reviewed to verify study eligibility. Dates of death were verified using the Social Security Death Index. Tissue samples from 23 low-grade gliomas (3 pilocytic astrocytomas, 4 grade II astrocytomas, 10 grade II oligodendrogliomas, and 6 grade II oligoastrocytomas) were collected. All samples used in this study were immediately flash frozen at the time of resection and were subsequently stored at -80°C until RNA extraction was performed.

Demographics

Demographic information for the 23 patients included in this study is summarized in Table 1. The patient population was 65% male and 35% female, and the mean age of patients at the time of surgical resection was 34.3 years (±4.66, 95% CI, range 10–60). Twenty tumors were supratentorial (87%) and three were infratentorial (13%). The surgical resection from which tissue used in this study was collected represented the first surgical intervention for 18 patients (79%), while 5 patients had undergone prior stereotactic biopsy (21%). Twenty patients were alive at the time of analysis (87%), and a censored survival point was entered for these patients. The mean survival (including censored survival) was 3.53 years (±0.59, 95% CI) from the time of diagnosis. The extent of resection in all patients was assessed on postoperative, contrast-enhanced MRI or CT imaging.

Extent of tumor resection

We defined gross total resection (GTR) as absence of residual lesional enhancement or MRI FLAIR abnormalities, near-total resection (NTR) as trace amounts of residual enhancement without obvious residual tumor mass (95–99% resection), and subtotal resection (STR) as obvious residual tumor mass, but with resection of >88% of original

Table 1
Demographics.

Number of patients (*n*)	23
Age (years) – mean	34.3
– 95% CI	4.7
Sex – M (%)	15 (65%)
– F (%)	8 (35%)
Location – supratentorial *n* (%)	20 (87%)
– Location – infratentorial *n* (%)	3 (13%)
Prior stereotactic biopsy – *n* (%)	5 (21%)
– *n* (%) GTR	12 (53%)
– *n* (%) NTR	6 (26%)
– *n* (%) STR	5 (21%)
Survival (censored, years) – Mean	3.53
– Survival (censored, years) – 95% CI	0.59
Alive at the time of analysis – *n* (%)	20 (87%)

CI: confidence interval; GTR: gross total resection; NTR: near total resection; STR: subtotal resection.

tumor. Using this definition, GTR was achieved in 12 (53%) of patients, NTR in 6 (26%), and STR in 5 (21%). Administration of adjuvant therapy was highly variable after resection, which reflects the variability of management protocols for patients with low-grade gliomas and which was not controlled for in this study.

Molecular genetic data

Data from molecular genetic assays routinely performed on brain tumor specimens at our institution were collected from the immunohistochemistry results reported in the anatomic pathology reports for all patients included in this study. Fluorescent *in situ* hybridization (FISH) demonstrated codeletion of chromosomes 1p and 19q in eight patients (35%), and one patient (4%) had a 19q deletion with an intact 1p. Chromosome 1p and 19q status was not informative in three (13%) and four (17%) patients, respectively, consistent with no allelic imbalance. The mean Ki-67 index, a descriptor for cellular proliferation reflecting the relative prevalence of the MKI67 protein, was 4.41 ($\pm$1.48, 95% CI). TP53 immunopositivity, a marker for the presence of TP53 mutations (where 0–10% staining represents the presence of wild-type p53 alleles and >10% staining represents the presence of mutated p53 alleles) was wild type in 10 patients (43%), mutated in 9 patients (39%), and was not recorded in 4 (17%) patients.

Molecular subgroup clinical data

The clinical data for the patients whose tumors comprise each of the identified molecular subgroups of glioma are summarized in Table 2. These subgroups are further discussed in Results and Discussion.

Gene expression analysis

Histologic verification of tumor cellularity and specimen quality was performed using frozen sections of the tumor blocks stained with hematoxylin and eosin. Gene expression analysis for the 23 tumors was performed following standard institutional protocols. Tissue extraction was performed using the TriZol® method, RNA was isolated and purified using Qiagen® column techniques, and quantification and quality assurance were performed using the NanoDrop® spectrophotometer and the Agilent® BioAnalyzer 2100, respectively. Microarray analysis was performed using the Affymetrix® U133 Plus 2.0 arrays and RT-PCR [28] was performed to confirm array data using the TAQMan assay, both following standard protocols. Data were analyzed using several commonly used software platforms for gene expression analysis, and gene list annotation was performed using data from multiple, publicly available annotation databases. Detailed descriptions of these methods are available in the supplemental materials.

Results

Molecular class discovery

Characterization of differentially expressed genes in tumors vs. controls

To characterize the genes that distinguished the low-grade gliomas group (as a whole) from normal brain, a two-sided *t*-test ($p<0.01$) with a standard Bonferroni correction was applied to the normalized dataset to identify a subset of 2021 genes with a high degree of statistically significant differential expression between tumor and normal brain (881 overexpressed, 1140 underexpressed, out of approximately 47,000 unique genes found on the Affymatrix U133A plus 2.0 array; see Supplemental materials). An EASE (Expression Analysis Systematic Explorer) [29] overrepresentation analysis was used to identify structural, functional, and pathway categories with statistically significant overrepresentation in the lists of differentially expressed genes. While the results for any specific category are difficult to interpret in isolation, this analysis gives an overall representation of the structural and functional categories that are differentially expressed among the tumor samples. The results of this analysis are included in the supplemental material, including a complete table of the identified genes (Table S1) and an abbreviated version listing only EASE categories with 100 or more hits (Table 2).

Table 2
Characteristics of molecular subgroups.

Age (years)	Survival (years)	Histology, WHO grade	Surgical outcome	Location	1P	19Q	Ki67 (%)	p53 (%)
Pilocytic astrocytoma (PA) cluster								
50	4.44	Microcystic astroctyoma, grade I	NTR	Temporal	I	I	1	10
24	4.01	Pilocytic astrocytoma, grade I	GTR	Cerebellar	NR	NR	2	NR
10	3.46	Pilocytic astrocytoma, grade I	GTR	Cerebellar	I	NR	5	NR
20	3.72	Pilocytic astrocytoma, grade I	GTR	Cerebellar	NR	NR	1	0
Codeleted oligodendroglioma (CO) cluster								
42	2.33	Oligodendroglioma, grade II	GTR	Frontal	D	D	5	0
42	5.08	Oligodendroglioma, grade II	NTR	Frontal	D	D	4	10
27	5.18	Oligodendroglioma, grade II	GTR	Frontal	D	D	3	NR
36	2.31	Oligodendroglioma, grade II	GTR	Frontal	D	D	3	10
28	1.70	Oligodendroglioma, grade II	STR	Temporal	D	D	9	3
36	1.83	Oligodendroglioma, grade II	GTR	Temporal	D	D	4	0
24	0.76	Oligodendroglioma, grade II	NTR	Parietal	D	D	12	2
38	6.15	Oligodendroglioma, grade II	GTR	Frontal	D	D	2	10
Residual low-grade gliomas								
21	5.48	Astrocytoma, grade II	NTR	Frontal	NR	NR	1.5	NR
60	2.41	Astrocytoma, grade II	STR	Temporal	I	I	1	5
22	2.69	Astrocytoma, grade II	STR	Frontal	I	I	10	50
38	3.05	Oligodendroglioma, grade II	GTR	Frontal	I	I	4	50
33	4.18	Oligodendroglioma, grade II	GTR	Parietal	I	I	10	75
32	5.59	Mixed glioma, grade II	GTR	Frontal	I	I	2	40
32	4.68	Mixed glioma, grade II	STR	Frontal	I	I	2	50
45	4.26	Mixed glioma, grade II	NTR	Temporal–parietal–occipital	I	I	1	75
43	3.39	Mixed glioma, grade II	NTR	Temporal	I	D	12	40
26	1.26	Mixed glioma, grade II	GTR	Temporal	I	I	5	50
37	3.17	Mixed glioma, grade II	STR	Frontal	I	I	2	50

GTR: gross total resection; NTR: near total resection; STR: subtotal resection;
D: deleted; I: intact; NR: not recorded.

Feature reduction for class discovery

Genes that are differentially expressed between the tumor and control populations serve as the basis for class discovery, while genes without statistically-significant differential expression do not make meaningful contributions to class discrimination and contribute only noise to clustering algorithms. Accordingly, a one class SAM (significance analysis for microarrays) [30] analysis (false discovery rate set to 0) was used to test the $\log_2\left(\frac{FI_{Tumor}}{FI_{AverageControl}}\right)$ for each gene against zero, identifying a subset of 19,876 genes with differential expression in the tumors relative to the control. This set of genes was used as the feature set for class discovery and clustering.

Molecular relationships among low-grade gliomas

Unsupervised analysis algorithms employ unbiased searches for patterns of expression that can be used to develop hypotheses regarding the mechanistic associations between genotype and phenotype. These approaches are useful to identify expression patterns within the set of differentially expressed genes that may have phenotypic significance. Hierarchical clustering [31] (Fig. 1) identified a cluster of four tumors that segregated at the most proximal level. Comparison to histopathologic diagnosis demonstrated that this cluster included all three pilocytic astrocytomas (PA) and one grade II astrocytoma (1p/19q intact). This fourth tumor was classified as grade II at the time of initial resection and pathologic review, but repeat histologic evaluation by our neuropathologist (RP) revealed a predominantly microcystic pattern; reanalysis confirmed that this lesion was a WHO grade I astrocytoma rather than its original, clinical pathology designation as a grade II, infiltrating glioma. Moreover, this patient's clinical course has more closely approximated that of a typical patient with a grade I glioma: the patient is alive 5 years after a near total resection and has no clinical or radiographic evidence of recurrence or progression. These finding lead us to conclude that the initial, histologic classification of this lesion as WHO grade II was erroneous and, in fact, this was a grade I astrocytoma. Proper reclassification was triggered by analysis of the microarray results. The PA cluster therefore comprises all four study patients with WHO grade I lesions.

A second, distinct cluster of eight tumors was identified during unbiased searching, which were found to be all oligodendrogliomas by histology. Comparison to chromosomal copy number data demonstrated that this cluster include eight of eight samples in the dataset with codeletion of chromosome 1p and 19q. The support tree algorithm [32] indicated 93% support for the pilocytic astrocytoma-like cluster (PA) and 95% support for the codeleted oligodendroglioma-like cluster (CO) (Fig. 1). Analysis of principal components [33] (Fig. 2A) and correspondence analysis [34,35] (Fig. 2B) were used to explore these relationships. These analyses revealed that the PA cluster segregated distinctly from the remainder of the tumors along both the first and the second principal components. The CO subset also clustered discretely along the first principal component. The remaining tumors, which represented a mixture of grade II astrocytomas, grade II mixed gliomas, and grade II oligodendrogliomas (1p/19q intact), formed a residual cluster whose members were distributed throughout the expression space and generally occupied the area at the margin of the CO cluster. This relationship was confirmed with terrain mapping [36] (with neighbors = 3, Fig. 3).

Characteristics of the identified molecular subgroups

PA cluster

The first molecular subgroup consisted of all four tumors identified as WHO grade I astroctyomas. The mean age of patients in this group was 26.0 years and the mean (censored) survival was 3.91 years, neither of which was significantly different from the corresponding values for the remaining groups (Table 2).

A two-group SAM analysis was used to determine the genes that were differentially expressed in this cluster versus the remaining

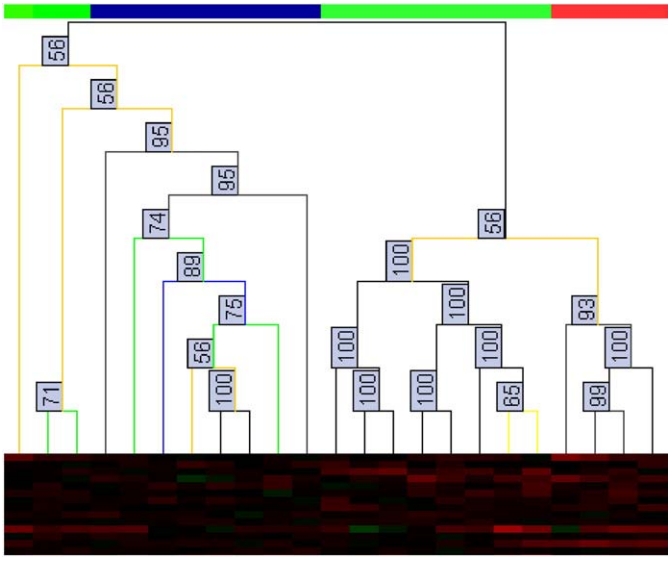

Fig. 1. Hierarchical clustering with support values. Red: PA cluster (Class I); blue: CO cluster (Class II); green: residual cluster (Class III). Numbers in grey boxes represent percent support for each node by the Support tree algorithm (Bootstrapping).

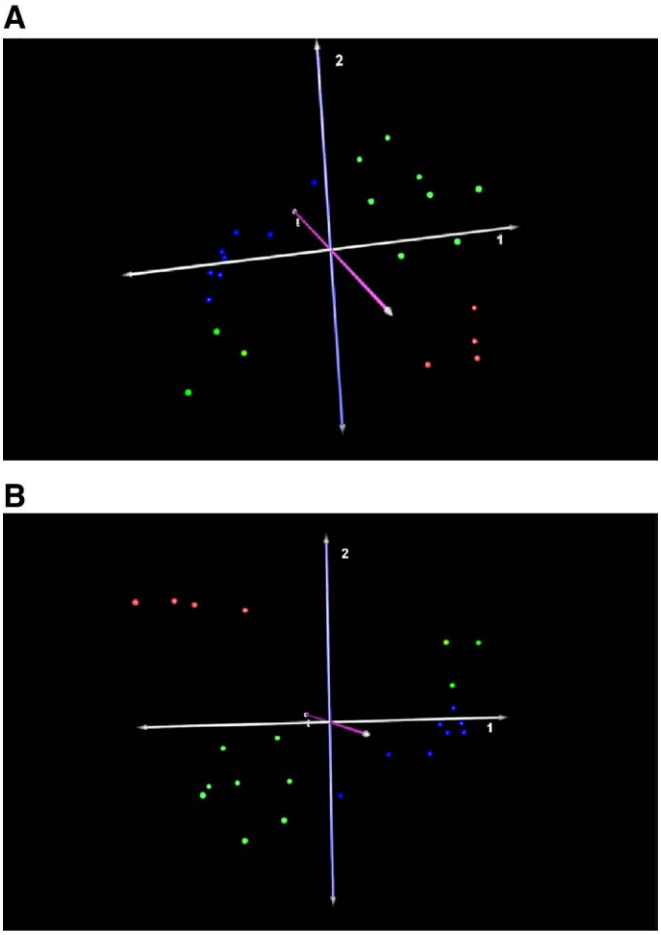

Fig. 2. Sample clustering by dimensional reduction. (A) Principal components analysis. (B) Correspondence analysis. Blue: CO cluster; red: PA cluster; green: residual cluster.

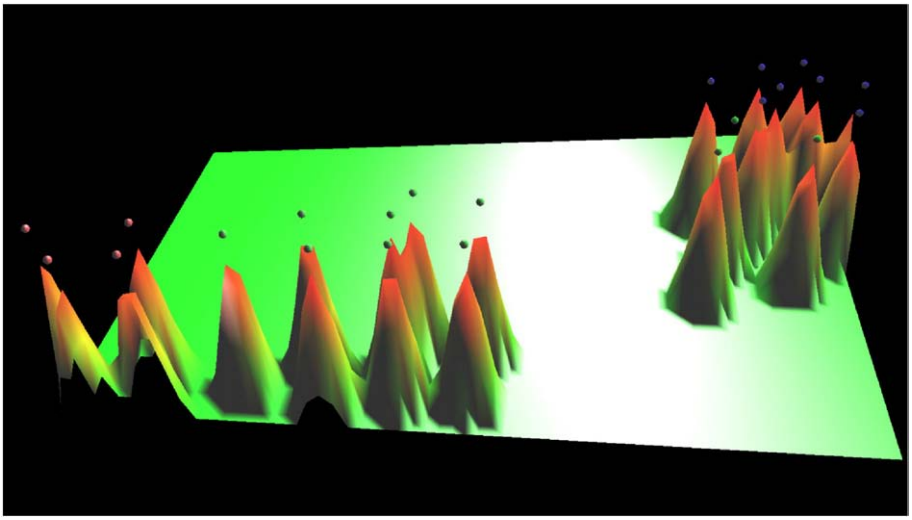

Fig. 3. Terrain mapping. Blue: CO cluster; red: PA cluster; green: residual cluster.

tumor population, as these genes are the discriminators of this molecular class. A total of 1367 genes with differential expression in this group were identified, with 1056 overexpressed in this group and 311 underexpressed relative to the remaining sample population. Chromosomal locus and functional category overrepresentation analysis was performed on these gene sets using EASE. The results demonstrate overexpression of genes localizing to chromosomes 5q, 7q, 8p, 11q, and 12 and underexpression of genes on chromosome 9q (Table 3). The results of the EASE overrepresentation analysis for these gene lists are included in the supplemental material (Table S3).

CO cluster

The second molecular subgroup consisted of eight tumors classified histologically as grade II oligodendrogliomas. Analysis of the molecular genetic data for these tumors demonstrated that this cluster represented 100% of the low-grade gliomas with chromosome 1p/19q codeletion. All eight of these tumors were supratentorial. The mean age of patients in this group was 34.1 years and the mean (censored) survival was 3.17 years, neither of which was significantly different from the corresponding values for the remaining groups (Table 2).

A two-group SAM analysis was used to determine the genes that were differentially expressed in this cluster versus the remaining tumor population. A total of 681 genes with differential expression in this group were identified, with 161 overexpressed and 520 underexpressed relative to the other 17 tumors. Chromosomal locus and functional category overrepresentation analysis revealed no chromosome-specific overrepresentation; there was underrepresentation of genes localizing to chromosomes 1p and 19q ($p<1.44\times10^{-59}$ and $p<0.009$, Table 3). The EASE overrepresentation analysis is included in the supplemental material (Table S4).

Table 3
Chromosomal overrepresentation analysis of molecular subgroups.

Category	Genes	EASE score
PA cluster, overrepresentation		
Chromosome 12	70	4.79E-10
Chromosome 12p	22	1.31E-04
Chromosome 12q	48	2.06E-06
Chromosome 8	30	0.035
Chromosome 8p	17	0.004
Chromosome 11	51	0.006
Chromosome 11q	34	0.024
Chromosome 7	39	0.026
Chromosome 7q	29	0.016
Chromosome 5	39	0.023
Chromosome 5q	34	0.018
PA cluster, underrepresentation		
Homo sapiens 9q	10	0.039
CO cluster, overrepresentation		
NONE		
CO cluster, underexpression		
Chromosome 1	133	1.92E-44
Chromosome 1p	115	1.44E-59
Chromosome 19q	24	0.009

Genes that distinguish between molecular subgroups

Identification and characterization of the PA and CO clusters gives rise to a three-class model of low-grade gliomas. Class I represents tumors in the PA cluster, class II corresponds to tumors in the CO cluster, and class III is a residual cluster containing the remaining tumor samples. Genes with distinct patterns of expression between each of these three molecular subgroups were identified using a three-class, one-way analysis of variance (ANOVA) with $p<0.01$ and a standard Bonferroni correction. This set of 304 genes was subsequently characterized with EASE overrepresentation analysis. Both the gene list and the EASE overrepresentation analysis are included in the supplemental material (Tables S5 and S7).

Prospective classification using machine learning models

Overview

Data sets where elements are members of known classes and where a large set of features is associated with each element can be used in conjunction with machine learning models to train prospective classifiers for novel elements having similar feature sets. Our unbiased class discovery strategy identified three distinct classes, and this knowledge was added to the expression data set and used to train mathematical learning models capable of classifying unknown tumors into one of these three classes based upon the expression profile. To build these models, we constructed a training set of two samples from the PA cluster, five samples from the CO cluster, and eight samples from the residual cluster to serve as a training set for subsequent classifiers. The remaining samples comprised the test set, consisting of two samples known to belong to the PA cluster, three from the CO cluster, and three from the residual cluster. Specific assignments to the training and test set were made at random.

Feature reduction for machine learning

Machine learning models represent a robust method of prospective classification, but the classification results can be affected by biases in the dataset. We used two strategies to control such potential bias. First, while knowledge of the group membership of the elements in the training set is used to train the classifier, information regarding the group assignment of elements in the test set is not introduced into the validation process and is examined only retrospectively after classification of the validation set. Next, feature reduction is performed on the complete expression data set using only variance filtering [37]. A variance filter was therefore applied to the complete, normalized expression dataset (54,676 genes) such that the least variable 30% (16,403) of genes were removed. This allows classification to be performed using those features most likely to facilitate classification [37], reduces noise in the algorithms, and does so in an unbiased fashion.

Classification of unknown samples by machine learning

Three machine learning models were trained and tested for prospective classification of low-grade gliomas. Discriminant analysis (DA) [38] is a multistep algorithm that first applies an ANOVA analysis on the dataset to select genes that should be near optimal for partitioning the unknown samples based upon permutations of gene expression in the training set. Next, a multivariate partial least squares (MPLS) method is used for gene dimensional reduction. This is followed by a polychotomous discriminant analysis (PDA). The training data were used to construct a DA classifier, and validation with the test set demonstrated classification of the unknown samples into the appropriate molecular classes with 100% accuracy. The list of 1049 genes and the EASE overrepresentation analysis of this list is included in the supplemental material (Tables S5 and S6).

A second strategy for classification is the recently described, uncorrelated shrunken centroids (USC) model [39]. This method was designed to allow prediction of phenotypic category of a tissue sample based upon its expression profile as well as identification of genes relevant to this classification. The USC method is based upon a shrunken centroids algorithm but modifies the approach by removing genes with highly similar expression patterns. This algorithm exploits the functional interdependence of genes to reduce the number of genes used for classification, which produces a smaller set of important genes and improves classification accuracy. Again, the training set was used to train the classifier, and validation with the test set demonstrated 100% accuracy in classification. While the USC model performed well, its dimensional reduction strategy resulted in the inclusion of a large number of ESTs and genes with hypothetical products in the final list. This can be observed when using this gene reduction algorithm with the Affymetrix® U133 Plus 2.0 arrays, and it explains the incomplete annotations of the USC lists in the supplemental material.

Support vector machines (SVM) [40] are perhaps the best known machine learning model. SVMs use known relationships between members of a subset of elements coupled with the expression patterns of all of the elements to create a training set of numeric weights for each element. In a second phase, the weights are used to assign discriminators to the elements, and a binary output results in elements being considered either “in or out” of the groups defined in the initial training process. The pattern of weights associated with each feature can be retained after training to give information regarding the genes used to construct the support vectors. Because SVMs are binary, the training and test sets must be adjusted to accommodate the model. We therefore divided the data into two subsets of samples, one representing the class II (the CO cluster) and one representing the remaining two classes (including both the residual and the PA cluster). Half of the samples in each subset ($4+8=12$) were selected at random to comprise the training set, and the other half ($4+7=11$) were used as the test set. Variance filtering was used (on previously unfiltered expression data) to select the most variable 5000 genes (9%) across these two groups to serve as the feature set for classification [37]. After training, the SVM classified the test set with 100% accuracy. A second round of SVM could theoretically be used to distinguish tumors in the PA class from the remainder of the data set (the implementation of a binary classifier in a multiclass model), but the small number of PAs precluded adequate training of a second round of SVM. The 2630 genes whose training weights favored the CO class and the 2370 weighted against the CO class, as well as the EASE overrepresentation analysis of these gene sets, are included in the supplemental material (Tables S6 and S7).

Verifying expression data

Reverse transcriptase-polymerase chain reaction (RT-PCR) was performed to validate the expression patterns in a subset of differentially expressed genes [28]. Six housekeeping genes were tested empirically. GAPDH was determined to be most consistent control and was used as the reference for all subsequent RT-PCR. Sixteen (16) genes that had been identified as having highly statistically significant differential expression between the three classes using three-way ANOVA or the Student's *t*-test were assayed in both controls and in all 23 samples, giving a total of 368 data points. These data were analyzed using three separate strategies — an ANOVA analysis, a relative analysis of gene expression across phenotypic groups, and a semiquantative analysis of differential gene expression.

The ANOVA analysis and the analysis of the relative expression patterns for each gene across the three phenotypic groups (PA, CO, and the residual gliomas) were performed using the mean RT-PCR fluorescence value for each gene in each phenotypic group (normalized to the GAPDH reference). A one-way, three-class ANOVA (adjusted $p<0.05$) confirmed statistically significant differential expression across the three phenotypic classes in nine genes (56.3%). The relative order of the magnitude of differential expression for each gene in each phenotypic group was examined and was compared to array data analyzed in a similar fashion. This analysis demonstrated that the relative order of gene expression was identical for 10 of the 16 genes (62.5%) in the array and the PCR analyses (Table S8).

A semiquantitative analysis of differential gene expression was performed by calculating the $\log_2$(ratio) of each gene in the PCR dataset relative to the mean the control value for the gene. Reliable control data were available for 10 of the 16 genes. These 10 genes in 23 samples were used for the semiquantitative analysis, resulting in a total of 230 data points. Internal controls in the RT-PCR system indicated that 227 of these points represented reliable data, and this dataset served as the basis for subsequent calculations. Analysis of the expression data for each of the 10 genes across all 23 samples demonstrated regulation in the same direction (either upregulation or downregulation) for a total of 139 of the 227 data points assayed (61.2%). Additionally, the RT-PCR and microarray data concurred on the direction of regulation in at least 50% of samples for 8 of the 10 assayed genes (80%). Analysis of these data by sample demonstrated concurrence of RT-PCR and microarray data for the direction of regulation in a mean of 60.4% of the genes in each sample. Forty (17.6%) of these data points demonstrated <50% difference in the measured magnitude of differential gene expression (relative to control), although comparisons of magnitude of differential regulation across platforms are subject to multiple sources of error and must be interpreted cautiously (Table S9).

Discussion

Demographic and clinical data

Table 1 summarizes the demographic data for the 23 patients in this investigation, and Table 2 presents relevant clinical data, including patient age and survival, location and characterization of

the brain lesions, a summary of surgical outcomes, and histologic and molecular pathologic data for each tumor. The difference in mean survival for the three clusters does not achieve statistical significance. This is likely attributable to a combination of the more indolent disease course characteristic of low-grade gliomas (>5-year survival) and the large number of censored survival values in our cohort (87%). Because of the potential biases associated with using censored data to analyze time to progression, we have not reported on this clinical parameter. Also, because management strategies for low-grade gliomas are highly variable – both from center to center and between patients in the same center – and because our sample size is relatively small, we have not commented on response to therapy (see supplemental discussion). Of note, while the sample size in this investigation is relatively small, it represents one of the largest, most comprehensive molecular investigations of low-grade gliomas reported to date [12,18–27].

Integrative analytic model

For many years, our understanding of the relationships among low-grade gliomas was based almost entirely upon histologic features, which are the basis of the WHO grading scheme. More recently, molecular differences among WHO grades I–II gliomas have been described [17,41] but the significance of many of these findings remains unclear. The most promising molecular data to date has come with the discovery and characterization of a subset of oligodendrogliomas with codeletions of chromosome 1p and 19q (principally a translocation of 1p to 19q), a molecular marker in otherwise histologically identical tumors that generally correlates with improved response to chemotherapy and prolonged survival relative to patients with 1p/19q intact tumors [42–44]. Findings such as this contribute to the case that molecular differences among histologically similar tumors may have phenotypic significance [9] but limited research into molecular relationships among low-grade gliomas has left much uncertainty regarding the number and nature of such molecular subclasses. The current WHO system does not include molecular classification data [1].

We intended to identify, in an unbiased fashion, the number and nature of molecular subgroups that exist among WHO grades I–II gliomas. The data analysis model we implemented is designed to integrate data from the genomic, transcriptomic, and morphologic domains so as to identify and characterize these molecular subgroups (Fig. 4). Once samples of low-grade gliomas are appropriately examined by an experienced neuropathologist (RP), molecular analyses are blinded to histologic information to eliminate potential bias. Preliminary class discovery is guided by unsupervised analysis of gene expression data, but final delineation of molecular classes is made through an integrative analysis of chromosomal, histologic, RT-PCR, and expression data. This structure also facilitates cross-validation of findings from each of the platforms (Fig. 4). Once molecular classes have been identified, this knowledge is used, along with expression data, in an unbiased fashion, to train prospective classifiers, and the classifiers are validated using expression profiles of novel tumors that were not part of the training set. Of primary importance in this model are the capability for intrinsic cross-validation and the integrative data analysis involved in class discovery.

Data cross-validation

Microarray expression data, RT-PCR data, and information on chromosomal copy number were cross-validated as outlined in Fig. 1.

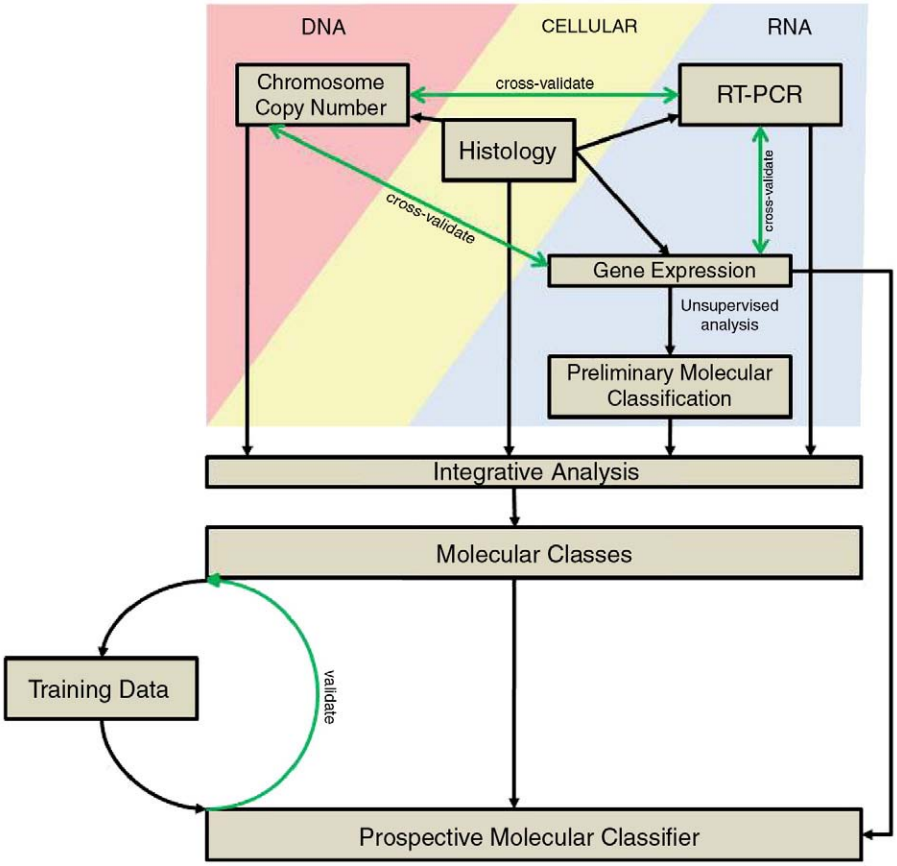

Fig. 4. Analytic model.

Genes identified as underexpressed in the CO cluster by microarray were annotated with chromosomal localization, and an EASE overrepresentation of this analysis demonstrated strong underexpression of genes localized to chromosomes 1p and 19q (Table 3). This matched the chromosomal copy number data, which demonstrated 1p/19q codeletion in all eight members of this cluster. Similar analysis of overexpressed genes in the PA cluster suggested overrepresentation of genes localizing to chromosomes 5q, 7q, 8p, 11q, and 12 (Table 3), and amplifications of all of these loci have been reported in the literature [45–50], most notably at 7q. We did not validate each of these potential copy number variations by whole-genome copy number analysis, but our data analysis model would accommodate such cross-validation as part of a more extensive study. Similarly, microarray and RT-PCR platforms were used to cross-validate measured gene expression levels. RT-PCR was performed on a subset of 16 genes with differential expression demonstrated by microarray analysis, and both a relative analysis of gene expression across phenotypic groups and a semiquantative analysis of differential gene expression supported the findings of the microarray analysis.

Three-class model for low-grade gliomas

The result of our integrative analysis for molecular class discovery is a three-class model for low-grade glioma classification. Class I, identified as the PA cluster, contains all of the samples histologically identified as WHO grade I lesions. This cluster is well supported in all class discovery algorithms and has gene expression signatures that are clearly distinct from the remainder of the low-grade gliomas. This subclassification is also consistent with general clinical characteristics of pilocytic astrocytomas, which, unlike other low-grade gliomas, tend to be circumscribed and noninfiltrative and are uniformly cured with gross total resection.

Class II, the CO cluster, represents a subset of low-grade gliomas found to have codeletion of chromosomes 1p and 19q by copy number analysis. This pattern of deletion is well described in the current literature [42–44]. By the WHO system, all of the tumors in this cluster, as well as two tumors in the residual cluster (class III), would be identified as oligodendrogliomas. Clinically, oligodendrogliomas with 1p/19q codeletion/translocations are infiltrative, but their response to current standard medical therapy and therefore their progression free survival rate is generally better than that of their 1p/19q intact counterparts.

Class III represents tumors not included in the PA or CO cluster. The expression patterns of these tumors are variable, and this cluster therefore appears on PCA and COA plots a “cloud” of samples distributed in multidimensional expression space. Clinically, this cluster represents a group of tumors with heterogeneous histology that are often considered as 1p/19q intact, low-grade, infiltrating gliomas. In general, such tumors are prone to progression and conversion to more malignant phenotypes. By the WHO system, this cluster is composed of a heterogeneous mix of non-pilocytic astrocytomas, some oligodendrogliomas, and mixed oligoastrocytomas.

Our model highlights potential areas for enhancing pathological classification nosologies for low-grade gliomas. While the WHO system does segregate pilocytic astrocytomas as distinct, 1p/19q deleted and 1p/19q intact oligodendrogliomas are grouped in a single category despite their divergent clinical performance and patterns of gene expression. Moreover, there are multiple WHO histological categories for the remaining low-grade gliomas (astrocytoma, oligodendroglioma, and oligoastrocytoma), which we have clustered together into class III. These tumors have similar patterns of gene expression and overlapping but not identical clinical behaviors. The biological relationships between tumor genotype and clinical phenotype in these tumors remain to be explored.

Clinical significance

The World Health Organization (WHO) grading system for glial tumors [1] provides at least eight classes for WHO grades I–II glial tumors. These classes are based purely upon histology; the WHO scheme does not use clinical or molecular data to develop these classes. By contrast, the three-class model that we have constructed is predicated upon molecular data from an integrated molecular analysis, and the identified classes correlate with current clinical paradigms regarding clinical behavior and management of low-grade gliomas. In our model, tumors with a profile similar to pilocytic astrocytomas are assigned to class I, infiltrative tumors similar to 1p/19q codeleted oligodendrogliomas are assigned to class II, and the remaining, infiltrative tumors are designated as class III. These three groups have distinct genotypes, both at the DNA and at the transcriptomic level. Similarly, current understanding of the clinical phenotypes of tumors assigned to these classes suggests that class I may represent tumors that are circumscribed and curable with resection, class II may reflect tumors that are infiltrating but respond favorably to current therapeutic modalities, and class III may be gliomas that may have an increased tendency toward treatment resistance, relative to class II tumors. This correlation between the three molecular classes and the three broad categories of clinical performance suggest that there may be a biological basis to the current clinical paradigm regarding the management of low-grade gliomas that is reflected in the transcriptome. Additionally, our findings suggest that molecular differences have the potential to serve as the basis for a clinically relevant classification scheme that may serve as a more accurate model to determine prognosis, to guide selection of therapeutic options, and to aid in the design of clinical trials, especially those that are expected to act on specific molecules or pathways. Additional information regarding potential limitations of this study – and future directions for research based upon the findings of this investigation – are detailed in the supplemental materials.

Conclusions

WHO grades I–II gliomas are a heterogeneous group of tumors whose histology, patterns of gene expression, phenotypes, and prognosis are variable. The goal of this study was to investigate, in an unbiased fashion, the number and nature of molecular subgroups that exist among these gliomas, and the data analysis model that we have implemented was designed to integrate data from the genomic, transcriptomic, and cellular levels for the purpose of identifying and characterizing these molecular subgroups. Our investigations suggest a three-class model for low-grade gliomas, where class I represents tumors with molecular similarity to pilocytic astrocytomas, class II represents gliomas with 1p/19q codeletions, and class III represents diffuse, infiltrating, low-grade gliomas. We have presented robust molecular data for our model. We believe that this classification may be a useful supplement to the current WHO grading scheme for low-grade gliomas.

Appendix A. Supplementary data

Supplementary data associated with this article can be found, in the online version, at doi:10.1016/j.ygeno.2009.09.007.

References

[1] D.N. Louis, H. Ohgaki, O.D. Wiestler, W.K. Cavenee (Eds.), WHO Classification of tumours of the central nervous system, IARC, Lyon, 2007.
[2] E.C. Holland, Glioblastoma multiforme: the terminator, Proc. Natl. Acad. Sci. U. S. A. 97 (2000) 6242–6244.
[3] E.A. Maher, F.B. Furnari, R.M. Bachoo, D.H. Rowitch, D.N. Louis, W.K. Cavenee, R.A. DePinho, Malignant glioma: genetics and biology of a grave matter, Genes Dev. 15 (2001) 1311–1333.

[4] M. Lacroix, D. Abi-Said, D.R. Fourney, et al., A multivariate analysis of 416 patients with glioblastoma multiforme: prognosis, extent of resection, and survival, J. Neurosurg. 95 (2001) 190–198.
[5] P.N. Kongkham, M. Bernstein, Low grade gliomas, in: M. Bernstein, M.S. Berger (Eds.), Neuro-oncology: The Essentials, 2nd ed., Thieme, New York, 2008.
[6] J.H. Rees, Low-grade gliomas in adults, Curr. Opin. Neurol. 15 (2002) 657–661.
[7] C.L. Ching, Genomic profiling in pediatric brain tumors, Cancer J. 11 (2005) 283–293.
[8] M.K. Sharma, D.B. Mansur, G. Reifenberger, A. Perry, J.F. Leonard, K.D. Aldape, M.G. Albin, R.J. Emnett, S. Loeser, M.A. Watson, R. Nagarajan, D.H. Gutmann, Distinct genetic signatures among pilocytic astrocytomas relate to their brain region origin, Cancer Res. 67 (2007) 890–900.
[9] N.F. Marko, S.A. Toms, G.H. Barnett, R. Weil, genomic expression patterns distinguish long term from short term glioblastoma survivors: a preliminary, feasibility study, Genomics 91 (2008) 395–406.
[10] S. Kim, E.R. Dougherty, I. Shmulevich, K.R. Hess, S.R. Hamilton, J.M. Trent, G.M. Fuller, W. Zhang, Identification of combination gene sets for glioma classification, Mol. Cancer Ther. 1 (2002) 1229–1236.
[11] R. Shai, T. Shi, T.J. Kremen, S. Horvath, L.M. Liau, T.F. Cloughesy, P.S. Mischel, S.F. Nelson, Gene expression profiling identifies molecular subtypes of gliomas, Oncogene 22 (2003) 4918–4923.
[12] S. Godard, G. Getz, M. Delorenzi, P. Farmer, H. Kobayashi, I. Desbaillets, M. Nozaki, A.C. Diserens, M.F. Hamou, P.Y. Dietrich, L. Regli, R.C. Janzer, P. Bucher, R. Stupp, N. de Tribolet, E. Domany, M.E. Hegi, Classification of human astrocytic gliomas on the basis of gene expression: a correlated group of genes with angiogenic activity emerges as a strong predictor of subtypes, Cancer Res. 63 (2003) 6613–6625.
[13] H.M. Fathallah-Shaykh, M. Rigen, L.J. Zhao, K. Bansal, B. He, H.H. Engelhard, L. Cerullo, K.V. Roenn, R. Byrne, L. Munoz, G.L. Rosseau, R. Glick, T. Lichtor, E. DiSavino, Mathematical modeling of noise and discovery of genetic expression classes in gliomas, Oncogene 21 (2002) 7164–7174.
[14] P.S. Mischel, R. Shai, T. Shi, S. Horvath, K.V. Lu, G. Choe, D. Seligson, T.J. Kremen, A. Palotie, L.M. Liau, T.F. Cloughesy, S.F. Nelson, Identification of molecular subtypes of glioblastoma by gene expression profiling, Oncogene 22 (2003) 2361–2373.
[15] C.L. Nutt, D.R. Mani, R.A. Betensky, P. Tamayo, J.G. Cairncross, C. Ladd, U. Pohl, C. Hartmann, M.E. McLaughlin, T.T. Batchelor, P.M. Black, A. Von Deimling, S.L. Pomeryo, T.R. Goulb, D.N. Louis, gene expression-based classification of malignant gliomas correlates better with survival than histological classification, Cancer Res. 63 (2003) 1602–1607.
[16] W.A. Freije, E. Castro-Vargas, Z. Fang, S. Horvath, T. Cloughesy, L.M. Liau, P.S. Mischel, S.F. Nelson, Gene expression profiling of gliomas strongly predicts survival, Cancer Res. 64 (2004) 6503–6510.
[17] S. Rorive, C. Maris, O. Debbeir, F. Sandras, M. Vidaud, I. Bieche, I. Salmon, C. Decaestecker, Exploring the distinctive biological characteristics of pilocytic and low-grade diffuse astrocytomas using microarray gene expression profiles, J. Neuropathol. Exp. Neurol. 65 (2006) 794–807.
[18] H. Huang, C. Stefano, M. Kurrer, Y. Yonekawa, P. Kleihues, H. Ohgaki, Gene expression profiling of low-grade diffuse astrocytomas by cDNA arrays, Cancer Res. 60 (2000) 6868–6874.
[19] S.L. Sallinen, P.K. Sallinen, H.K. Haapasalo, J.H. Helin, P.T. Helen, P. Schraml, O.P. Kallioniemi, J. Kononen, Identification of differentially expressed genes in human gliomas by DNA microarray and tissue chip techniques, Cancer Res. 60 (2000) 6617–6622.
[20] S. Hunter, A. Young, J. Olson, D.J. Brat, G. Bowers, J.N. Wilcox, D. Jaye, S. Mendrinos, A. Neish, Differential expression between pilocytic and anaplastic astrocytomas: identification of apolipoprotein D as a marker for low-grade, non-infiltrating primary CNS neoplasms, J. Neuropathol. Exp. Neurol. 61 (2002) 275–281.
[21] D.S. Rickman, M.P. Bobek, D.E. Misek, R. Kuick, M. Blaivas, D.M. Kurnit, J. Taylor, S.M. Hanash, Distinctive molecular profiles of high-grade and low-grade gliomas based on oligonucleotide microarray analysis, Cancer Res. 18 (2001) 6885–6891.
[22] D.H. Gutmann, N.M. Hedrick, J. Li, R. Nagarajan, A. Perry, M.A. Watson, Comparative gene expression profile analysis of neurofibromatosis 1-associated and sporadic pilocytic astrocytomas, Cancer Res. 62 (2002) 2085–2091.
[23] S. Khatua, K.M. Peterson, K.M. Brown, C. Lawlor, M.R. Santi, B. LaFleur, D. Dressman, D.A. Stephan, T.J. MacDonald, Overexpression of the EGFR/FKBP12/HIF-2alpha pathway identified in childhood astrocytomas by angiogenesis gene profiling, Cancer Res. 63 (2003) 1865–1870.
[24] J.Y. Ljubimova, A.J. Lakhter, A. Loksh, W.H. Yong, M.S. Reidinger, J.H. Miner, L.M. Sorokin, A.V. Ljubimov, K.L. Black, Overexpression of alpha4 chain-containing laminins in human glial tumors identified by gene microarray analysis, Cancer Res. 61 (2001) 5010–5061.
[25] J. van den Boom, M. Wolter, R. Kuick, D.E. Misek, A.S. Youkilis, D.S. Wechsler, C. Sommer, G. Reifenberger, S.M. Hanash, Characterization of gene expression profiles associated with glioma progression using oligonucleotide-based microarray analysis and real-time reverse transcription-polymerase chain reaction, Am. J. Pathol. 163 (2003) 1033–1043.
[26] K.K. Wong, Y.M. Chang, Y.T. Tsang, L. Perlaks, J. Su, A. Adesina, D.L. Armstrong, M. Bhattacharjee, R. Dauser, S.M. Blaney, M. Chintagumpala, C.C. Lau, Expression analysis of juvenile pilocytic astrocytomas by oligonucleotide microarray reveals two potential subgroups, Cancer Res. 65 (2005) 76–84.
[27] H. Huang, A. Hara, T. Homma, Y. Yonekawa, H. Ohgaki, Altered expression of immune defense genes in pilocytic astrocytomas, J. Neuropathol. Exp. Neurol. 64 (2005) 891–901.
[28] S.A. Bustin, Absolute quantification of mRNA using real-time reverse transcription polymerase chain reaction assays, J. Mol. Endocrinol. 25 (2000) 169–193.
[29] D.A. Hosack, G. Dennis, B.T. Sherman, C.H. Lane, R.A. Lempicki, Identifying biological themes within lists of genes with EASE, Genome Biol. 4 (2003) P4.
[30] V.G. Tusher, R. Tibshirani, G. Chu, Significance analysis of microarrays applied to the ionizing radiation response, Proc. Natl. Acad. Sci. U. S. A. 98 (2001) 5116–5121.
[31] M.B. Eisen, P.T. Spellman, P.O. Brown, D. Botstein, Cluster analysis and display of genome-wide expression patterns, Proc. Natl. Acad. Sci. U. S. A. 95 (1998) 14863–14868.
[32] D. Graur, W.H. Li, Fundamentals of Molecular Evolution, 2nd ed., Sinauer Assoc, Sunderland, MA, 2000, pp. 209–210.
[33] S. Raychaudhuri, J.M. Stuart, R.B. Altman, Principal components analysis to summarize microarray experiments: application to sporulation time series, Pac. Symp. Biocomput. (2000) 455–466.
[34] K. Fellenberg, N.C. Hauser, B. Brors, A. Neutzner, J.D. Hoheisel, M. Vingron, Correspondence analysis applied to microarray data, PNAS 98 (2001) 10781–10786.
[35] A.C. Culhane, G. Perriere, E.C. Considine, T.G. Cotter, D.G. Higgins, Between-group analysis of microarray data, Bioinformatics 18 (2002) 1600–1608.
[36] S.K. Kim, J. Lund, M. Kiraly, K. Duke, M. Jiang, J.M. Stuart, A. Eizinger, B.N. Wylie, G.S. Davidson, A gene expression map for *Caenorhabditis elegans*, Science 293 (2001) 2087–2092.
[37] C. Sima, U. Braga-Neto, E.R. Dougherty, Superior feature-set ranking for small samples using bolstered error estimation, Bioinformatics 21 (2005) 1054–1064.
[38] D.V. Nguyen, D.M. Rocke, Multi-class cancer classification via partial least squares with gene expression profiles, Bioinformatics 18 (9) (2002) 1216–1226.
[39] K.Y. Yeung, Bumgarner RE. 2003 Multiclass classification of microarray data with repeated measurements: application to cancer, Genome Biol. 4 (12) (2003) R83.
[40] M.P. Brown, W.N. Grundy, D. Lin, N. Cristianini, C.W. Sugnet, T.S. Furey, M. Ares Jr, D. Haussler, Knowledge-based analysis of microarray gene expression data by using support vector machines, Proc. Natl. Acad. Sci. U. S. A. 97 (2000) 262–267.
[41] K. Aldape, P.C. Burger, A. Perry, Clinicopathologic aspects of 1p/19q loss and the diagnosis of oligodendroglioma, Arch. Pathol. Lab. Med. 131 (2007) 242–251.
[42] J.G. Cairncross, D.R. Macdonald, Successful chemotherapy for recurrent malignant oligodendroglioma, Ann. Neurol. 23 (1998) 360–364.
[43] R.B. Jenkins, H. Blair, K.V. Ballman, C. Giannini, R.M. Arusell, M. Law, H. Flynn, S. Passe, S. Felten, P.D. Brown, E.G. Shaw, J.C. Buckner, A t(1;19)(q10;p10) mediates the combined deletions of 1p and 19q and predicts a better prognosis of patients with oligodendroglioma, Cancer Res. 66 (2006) 9852–9861.
[44] C. Giannini, P.C. Burger, B.A. Berkey, J.G. Cairncross, R.B. Jenkins, M. Mehta, W.J. Curran, K. Aldape, Anaplastic oligodendroglial tumors: refining the correlation among histopathology, 1p 19q deletion and clinical outcome in Intergroup Radiation Therapy Oncology Group Trial 9402, Brain Pathol. 18 (2008) 360–369.
[45] U. Fischer, A. Keller, P. Leidinger, S. Deutscher, S. Heisel, S. Urbschat, H. Lenhof, E. A. Meese, Different view on DNA amplifications indicates frequent, highly complex, and stable amplicons on 12q13-12 in glioma, Mol. Cancer Res. 6 (2008) 576–584.
[46] J. Szymas, G. Wolf, S. Petersen, K. Schluens, S. Nowak, I. Petersen, Comparative genomic hybridization indicating two distinct subgroups of pilocytic astrocytomas, Neurosurg. Focus 8 (4) (2000).
[47] F.V. White, D.C. Anthony, E.J. Yunis, N.J. Tarbell, R.M. Scott, D.E. Schofield, Nonrandom chromosomal gains in pilocytic astrocytomas of childhood, Hum. Pathol. 26 (1995) 979–986.
[48] D.T. Jones, K. Ichimura, L. Liu, D.M. Pearson, K. Plant, V.P. Collins, Genomic analysis of piolcytic astrocytomas at 0.97 Mb resolution shows an increasing tendency toward chromosomal copy number with age, J. Neurpathol. Exp. Neurol. 65 (2006) 1049–1058.
[49] R.N. Wiltshire, J.E. Herndon, A. Lloyd, H.S. Friedman, D.D. Bigner, S.H. Bigner, R.E. McLendon, Comparative Genomic Hybridization analysis of astroctyomas: prognostic and diagnostic implications, J. Mol. Diagn. 6 (2004) 166–179.
[50] S.H. Bigner, R.E. McLendon, H. Fuchs, P.E. McKeever, H.S. Friedman, Chromosomal characterization of childhood brain tumors, Cancer Genet. Cytogenet. 97 (1997) 125–134.